Volume 11
Number 27
21 July 2020
Pages 4347-4522

Polymer Chemistry

rsc.li/polymers

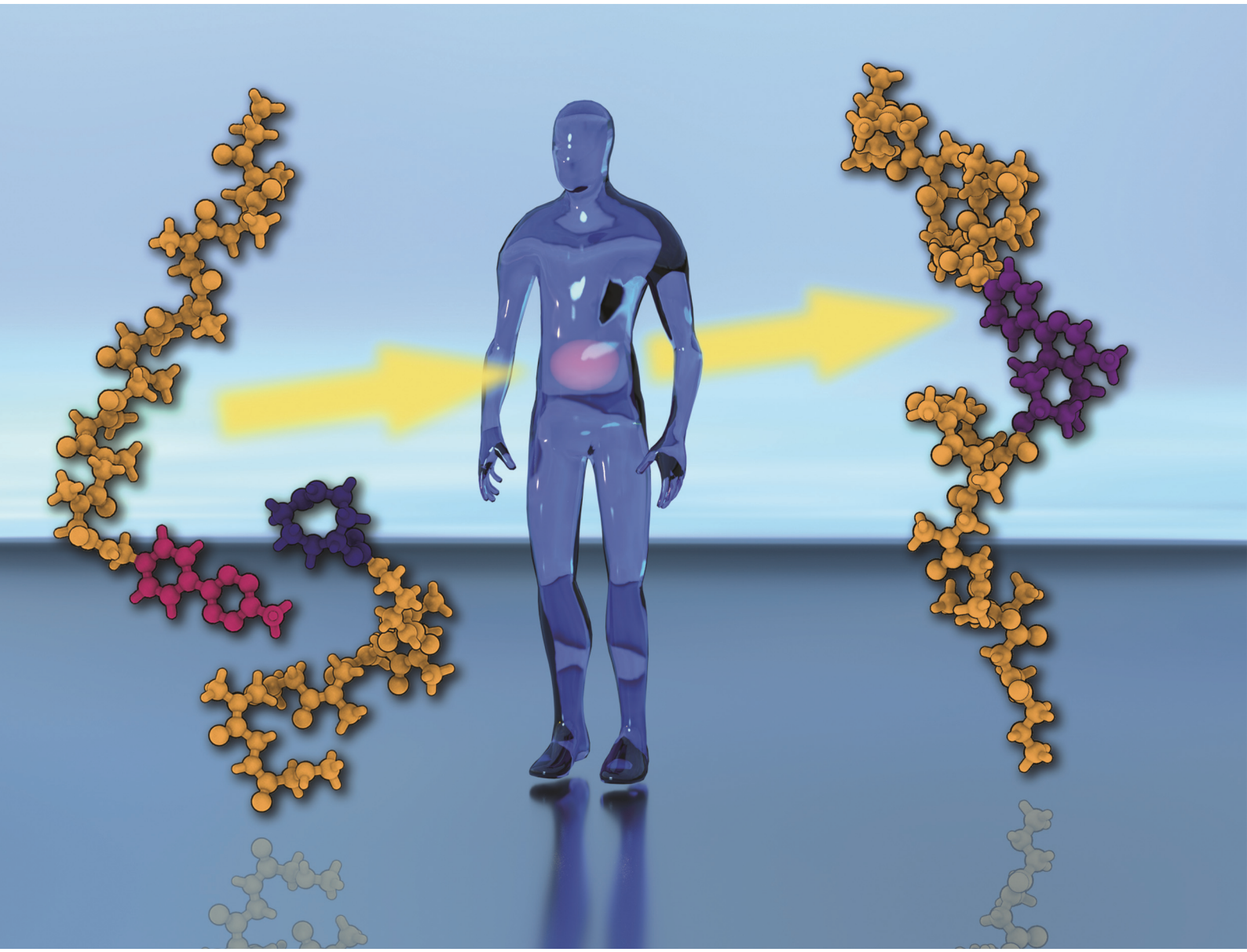

ISSN 1759-9962

ROYAL SOCIETY OF CHEMISTRY

PAPER

Matthias Barz *et al.*

Tetrazine- and *trans*-cyclooctene-functionalised polypept(o)ides for fast bioorthogonal tetrazine ligation

Polymer Chemistry

ROYAL SOCIETY OF CHEMISTRY

PAPER

View Article Online
View Journal | View Issue

Cite this: *Polym. Chem.*, 2020, **11**, 4396

Tetrazine- and *trans*-cyclooctene-functionalised polypept(o)ides for fast bioorthogonal tetrazine ligation†

Kerstin Johann,[a] Dennis Svatunek,[b] Christine Seidl,[a] Silvia Rizzelli,[a] Tobias A. Bauer,[a] Lydia Braun,[a] Kaloian Koynov,[c] Hannes Mikula[b] and Matthias Barz*[a]

The inverse electron demand Diels–Alder (IEDDA) reaction-initiated ligation between 1,2,4,5-tetrazines (Tz) and *trans*-cyclooctenes (TCO) is one of the fastest bioorthogonal reactions known today and is therefore increasingly used for *in vivo* click chemistry. Described herein is the synthesis of Tz- and TCO-functionalised polypeptides, polypeptoids and polypeptide-*block*-polypeptoids (polypept(o)ides) by ring-opening polymerisation of the corresponding *N*-carboxyanhydrides using Tz- or TCO-functional amine initiators. Despite the reactivity of tetrazines, polymers with low dispersity and high end group integrity can be obtained as observed by gel permeation chromatography (GPC), nuclear magnetic resonance (NMR) spectroscopy and matrix-assisted laser desorption/ionization time-of-flight (MALDI-TOF) mass spectrometry. Amphiphilic Tz-functionalised block copolypept(o)ides were used to prepare polymeric micelles and organic colloids by miniemulsion techniques, which may find an application as clearing agents in pretargeted nuclear imaging and therapy using efficient *in vivo* click chemistry. The reaction kinetics of the tetrazine ligation using the synthesised polymers and the accessibility of the Tz groups on the polymeric nanoparticles were evaluated using UV–Vis and fluorescence correlation spectroscopy (FCS), and second-order rate constants were determined by stopped-flow spectrophotometry ensuring quantitative conversions in seconds at sub-millimolar concentrations (10–30 s).

Received 12th March 2020,
Accepted 27th April 2020

DOI: 10.1039/d0py00375a

rsc.li/polymers

Introduction

In the last decade, the development of fast chemoselective reactions for efficient labelling of molecules *in vitro* and also *in vivo*, so-called bioorthogonal reactions, has seen significant advances.[1] Bertozzi *et al.* were the first to show that the bioorthogonal reaction between azides and alkynes can be accelerated by using strained reactants.[2] In 2008, the Fox and Weissleder lab independently reported on the inverse electron demand Diels–Alder (IEDDA) reaction of 1,2,4,5-tetrazines (Tz) with strained alkenes as fast bioorthogonal reactions for *in vivo* click chemistry.[3] This type of reaction has since been intensively investigated and the reactants have been further optimized in order to increase the rates of the reaction while retaining stability under physiological conditions.[4,5] Today, the fastest known click reactions occur between Tz and *trans*-cyclooctenes (TCO) with second-order rate constants of up to 3.3×10^6 M^{-1} s^{-1} and between Tz and *trans*-1-sila-4-cycloheptene with $k_2 = 1.14 \times 10^7$ M^{-1} s^{-1}.[4,6] It is therefore not surprising that the tetrazine ligation has been increasingly used in biomedical research, for example in pretargeting strategies,[7,8] in peptide chemistry,[9] for site-specific labelling of proteins,[10] as bioorthogonal cell glue[11] or for triggered drug release *via* "click-to-release" chemistry.[12]

With regard to the use of IEDDA reactions in polymer chemistry, the Tz-norbornene reaction was for example utilised for the post-polymerisation functionalisation of norbornene-functionalised polylactide[13] and poly(carbonate)s[14] or polymer–polymer coupling of poly(ethylene glycol) (PEG)-Tz and polystyrene-norbornene.[15] The Tz-TCO ligation, however, has not been widely used in the field of polymer science yet. This reaction has for instance been employed for site-selective

[a]*Department of Chemistry, Johannes Gutenberg University Mainz, Duesbergweg 10-14, 55128 Mainz, Germany. E-mail: barz@uni-mainz.de*
[b]*Institute of Applied Synthetic Chemistry, Technische Universität Wien, Getreidemarkt 9, 1060 Vienna, Austria*
[c]*Max Planck Institute for Polymer Research, Ackermannweg 10, 55128 Mainz, Germany*

†Electronic supplementary information (ESI) available: Procedures of the monomer synthesis, additional reaction schemes and structures, supplementary NMR, MALDI-TOF and UV–Vis spectra and GPC elugrams. See DOI: 10.1039/d0py00375a

protein modification,[16] to synthesise homodimeric protein-polymer conjugates[17] or for surface functionalisation.[18] Furthermore, Tz-modified dextran polymers have been applied in pretargeted nuclear imaging approaches using the tetrazine ligation, both as a secondary imaging agent and as masking agent.[19,20] Clearing agents for pretargeting strategies have also been prepared using Tz-functionalised albumin and polystyrene beads with albumin-Tz coating.[21] Kara *et al.* developed a synthetic approach for direct tetrazine synthesis on the backbone of poly(*N*-isopropyl acrylamide) (PNIPAAm) and PEG-based polymers.[22] Recently, Kramer *et al.* synthesised *N*-(2-hydroxypropyl)methacrylamide (HPMA)-based block copolymers functionalised with Tz groups either at the chain end by using a Tz-functional chain transfer agent or randomly distributed by post-polymerisation modification.[23] In a recent work, we developed TCO-functionalised molecular polymer brushes (PeptoBrushes), polypeptide-*graft*-polypeptoid polymers functionalised with multiple TCO groups, as tumour targeting agents for pretargeted nuclear imaging.[8]

While polypeptides are an established class of polymer materials,[24,25] polypeptoids[26,27] and polypept(o)ides[28] are just recently investigated in greater detail. Polypept(o)ides, hybrid materials combining polypeptides with the polypeptoid polysarcosine (pSar; poly(*N*-methylated glycine)), combine chemical versatility with high biocompatibility, which seems to be particularly interesting for applications in nanomedicine.[29,30] Both polypeptides and polypeptoids can be conveniently synthesised by ring-opening *N*-carboxyanhydride (NCA) polymerisation yielding polymers with narrow molecular weight distributions and with the possibility to introduce functional end groups by the use of functional initiators.[31–33] The non-ionic, hydrophilic pSar has shown stealth-like properties comparable to those of PEG, *i.e.* high solubility in water and low cellular toxicity and immunogenicity in various preclinical models.[8,27,30,34,35] It represents exclusively an H-bond acceptor without donor properties and thus follows the Whitesides' rules for protein resistant materials.[36] In contrast, polypeptides can also be of anionic, cationic or hydrophobic nature. They can be stimuli-responsive, biodegradable and undergo secondary structure-directed self-assembly in solution.[25,37] We previously reported on the synthesis of end group functionalised polysarcosine and polypeptides for the application in copper(I)-catalysed azide–alkyne coupling (CuAAC), strain-promoted azide–alkyne coupling (SPAAC) and native chemical ligation (NCL).[33]

In this work, we describe the straightforward synthesis of Tz- and TCO-functionalised pSar, poly(γ-benzyl-L-glutamate) (pGlu(OBn)) and the amphiphilic block copolypept(o)ide pSar-*block*-pGlu(OBn), by using the respective functional initiators, as well as their use in the tetrazine ligation. Polymeric micelles and organic colloids based on poly(D,L-lactide) were also prepared from Tz-pSar-*block*-pGlu(OBn). It will be demonstrated that the Tz groups preserve their reactivity and can be used for efficient functionalisation of the synthesised polymers, block copolymer synthesis and the functionalisation of polymeric nanoparticles.

Experimentals

Materials and methods

Materials. All reagents and solvents were purchased from Acros Organics (Nidderau, Germany), Sigma Aldrich (Munich, Germany), Roth (Karlsruhe, Germany) or Fluka (Munich, Germany) and used as received unless otherwise noted. Tetrahydrofuran (THF) and *n*-hexane were dried over sodium prior to use. Diethyl ether was distilled to remove the stabilizer. Dry *N*,*N*-dimethylformamide (DMF) over molecular sieves was purchased from Acros. Prior to use, DMF was degassed by three freeze–pump–thaw cycles to remove residual dimethylamine. *N*,*N*-Diisopropylethylamine (DIPEA) was purchased from Roth, dried over sodium hydroxide and fractionally distilled on molecular sieves. Diphosgene and sarcosine were purchased from Alfa Aesar. H-Glu(OBn)-OH was purchased from ORPEGEN Peptide Chemicals GmbH (Heidelberg, Germany). 4-((6-Methyl-1,2,4,5-tetrazin-3-yl)phenyl) methanamine (6-methyl-tetrazine-amine; mTz-NH_2) HCl salt and (*E*)-cyclooct-4-en-1-yl (3-aminopropyl)carbamate (*trans*-cyclooctene-amine; TCO-NH_2) HCl salt were obtained from Jena Bioscience (Jena, Germany). Poly(D,L-lactide) (PDLLA, M_w = 18 000–28 000 g mol^{-1}) was purchased from Sigma Aldrich. Deuterated solvents were obtained from Deutero GmbH (Kastellaun, Germany). Milli-Q (MP) water (Millipore) with a resistance of 18.2 MΩ and TOC <3 ppm was used throughout the experiments. Dialysis was performed with Spectra/Por membranes (Roth) with a nominal molecular weight cut-off of 3500 g mol^{-1}. Cy5-TCO was purchased from Click Chemistry Tools (Scottsdale, Arizona, US).

Methods. 400 MHz ^{1}H NMR and diffusion-ordered spectra were recorded on a Bruker Avance III HD 400 spectrometer at room temperature. All spectra were referenced to the solvent residual signals. The analysis of ^{1}H NMR spectra was performed using the software MestReNova v12.0.0 (Mestrelab Research S.L.).

Analytical hexafluoroisopropanol (HFIP) gel permeation chromatography (GPC) was carried out at a flow rate of 0.8 mL min^{-1} at 40 °C with 3 g L^{-1} potassium trifluoroacetate added to the eluent. The GPC system was equipped with a UV detector (Jasco UV-2075 Plus) set at a wavelength of 230 nm and an RI detector (Jasco RI-2031). Modified silica gel columns (PFG columns, particle size: 7 μm, porosity: 100 Å and 4000 Å) were used. Molecular weights were determined by using a calibration with poly(methyl methacrylate) (PMMA) standards (Polymer Standards Service GmbH Mainz) and toluene as an internal standard. The degree of polymerisation (DP) of polysarcosine (pSar) was determined by calibration of apparent M_n against a series of pSar standards characterised by static light scattering to obtain absolute molecular weights.[34] Prior to measurement, the samples were filtered through polytetrafluoroethylene (PTFE) syringe filters with a pore size of 0.2 μm. The elution diagram was analysed with WinGPC software (Polymer Standards Service GmbH Mainz).

Attenuated total reflectance Fourier transform infrared (ATR-FTIR) spectroscopy was performed on an FT/IR-4100

(JASCO Corporation) with an ATR sampling accessory (MIRacleTM, Pike Technologies). The IR spectra were analysed with the software Spectra Manager version 2.02.05 (JASCO Corporation). 16 scans were performed per measurement.

Single-angle dynamic light scattering (DLS) measurements were performed on a Zetasizer Nano ZS (Malvern Instruments Ltd, Worcestershire, UK) at an angle of 173° and a wavelength of 633 nm at 25 °C. Three measurements were performed per sample at a concentration of 0.3 mg mL^{-1} in 10 mM NaCl solution, and size distribution (intensity-weighted) histograms were calculated based on the autocorrelation function of samples, with automated attenuator adjustment and multiple scans (typically 10–15 scans). For the analysis of the data, Malvern Zetasizer Software version 7.12 was used.

Ultraviolet–visible (UV–Vis) spectroscopy was carried out on a Jasco V-630 spectrophotometer. The UV–Vis spectra were analysed with the software Spectra Manager version 2.07.02 (JASCO Corporation).

Melting points were measured using a Mettler FP62 melting point apparatus at a heating rate of 1 °C min^{-1}.

Reaction kinetics of Tz-polymers with PEG_4-TCO were determined using pseudo-first-order measurements with an excess of PEG_4-TCO in PBS (pH = 7.4) at 37.0 ± 0.1 °C following the decrease of tetrazine absorbance at 535 nm. Measurements were performed in triplicates using an SX20 stopped-flow photometer (Applied Photophysics, UK) equipped with a 535 nm LED light source. Data analysis was performed using Prism 6 (Graphpad) to determine the observed rate constants which were converted into second-order rate constants through dividing by the TCO concentration. Reaction kinetics of the reference compounds HELIOS 347Me and HELIOS 388Me with PEG_4-TCO or TCO-polymers were determined using pseudo-first-order measurements with an excess of the TCO compound in PBS (pH = 7.4) at 37.0 ± 0.1 °C following the increase of fluorescence at >400 nm. Measurements were performed in triplicates using an SX20 stopped-flow photometer (Applied Photophysics, UK) equipped with a 360 nm LED light source and a photomultiplier type R374 in combination with a 400 nm longpass filter as detector. Data analysis was performed using Prism 6 (Graphpad) to determine the observed rate constants which were converted into second-order rate constants through dividing by the TCO concentration. The used concentrations, observed rate constants and calculated second-order rate constants are shown in Table 2.

MALDI-TOF mass spectra were recorded on a Shimadzu Axima CFR MALDI-TOF mass spectrometer equipped with a nitrogen laser delivering 3 ns pulses at a wavelength of 337 nm or on a Bruker rapifleX MALDI-TOF/TOF mass spectrometer equipped with a 10 kHz scanning smartbeam 3D laser. HABA (2-(4′-hydroxybenzeneazo)benzoic acid) or dithranol were used as matrices for pSar or pGlu(OBn) respectively. Samples were prepared by dissolving the polymer in methanol or dichloromethane at a concentration of 1 mg mL^{-1}. 10 μL of the sample solution and 10 μL of matrix solution (10 mg mL^{-1}) in methanol or dichloromethane were added to a multistage target and the solvents were evaporated to create a thin matrix/analyte film. The samples were measured in linear or reflectron mode and analysed using mMass software version 5.5.0. Additionally, spectra were analysed using MATLAB. After baseline correction and peak assignment, dispersities of the molecular weight distribution were calculated for each polymer.

Fluorescence correlation spectroscopy (FCS) experiments were performed using a commercial FCS setup (Zeiss, Germany) consisting of the module ConfoCor 2 and an inverted microscope model Axiovert 200 with a Zeiss C-Apochromat 40×/1.2 W water immersion objective. The excitation was done by the 633 nm spectral line of a He/Ne laser and the collected fluorescence was filtered through an LP650 long pass emission filter before reaching the detector, an avalanche photodiode that enables single-photon counting. Eight-well polystyrene-chambered coverglass (Laboratory-Tek, Nalge Nunc International) was used as a sample cell. For each solution, a series of 10 measurements with a total duration of 5 min were performed. The obtained experimental autocorrelation curves were fitted with the theoretical model function for an ensemble of m different types of freely diffusing fluorescence species. The fits yielded the diffusion times of the fluorescent species from which the respective diffusion coefficients were evaluated.[38] Finally, the hydrodynamic radii (R_h) were calculated (assuming spherical particles) by using the Stokes–Einstein relation:

$$R_h = \frac{k_B T}{6\pi\eta D}$$

In this equation, k_B is the Boltzmann constant, T is the temperature, D the diffusion coefficient and η is the viscosity of water. A reference standard with known diffusion coefficient (Alexa Fluor 647) was used for calibration.

Scanning electron microscopy (SEM) images were recorded on a field emission microscope (LEO 1530 Gemini) working at an acceleration voltage of 0.7 kV. Samples were dried on a silica wafer at a concentration of approximately 0.1 mg mL^{-1}. The images were analysed using ImageJ.

Atomic force microscopy (AFM) images were obtained on a Cypher AFM (Asylum Research) at a scan rate of 1.0 Hz. Samples were prepared by placing a drop of the particle solution with a concentration of approximately 0.1 mg mL^{-1} onto freshly cleaned mica. The recorded images were analysed using Gwyddion software, version 2.49.

Synthetic procedures

Synthesis of sarcosine *N*-carboxyanhydride (NCA) and γ-benzyl-L-glutamate NCA. NCAs were synthesised as previously reported.[31] See ESI† for a detailed description of the syntheses.

General procedure for the synthesis of mTz-polysarcosine (mTz-pSar) using the example of mTz-$pSar_{101}$. The synthesis of mTz-pSar was carried out in a similar way as previously described for polysarcosine.[31] mTz-NH_2 HCl salt (36.4 mg) was weighed into a pre-dried Schlenk-tube to which 2 mL benzene were added for azeotropic removal of water. After stirring for 30 min the solvent was removed under reduced pressure and the initiator was additionally dried in high vacuum for 1 h.

Then, a stock solution was prepared by adding 2 mL dry DMF and 29.3 μL (1.1 eq. in relation to mTz-NH_2) DIPEA to deprotonate the amine group. Sar NCA (225 mg, 1.95 mmol) was transferred into a pre-dried Schlenk-tube equipped with a stir bar under nitrogen counter flow and dried in high vacuum for 1 h prior to reaction. The NCA was dissolved in anhydrous DMF (1 mL) and 1.02 mL of the stock solution of the initiator were added against nitrogen counter-flow. The solution was stirred overnight at room temperature (RT) and kept at a constant pressure of 1.25 bar of dry nitrogen *via* the Schlenk-line. Completion of the reaction was confirmed by IR spectroscopy (disappearance of the carbonyl stretching vibration bands at 1850 and 1780 cm^{-1}). The polymer was precipitated into diethyl ether and centrifuged (4500 rpm at 4 °C for 10 min). After discarding the liquid fraction, additional diethyl ether was added and the polymer was re-suspended in a sonication bath. The suspension was centrifuged again and the procedure was repeated once more. After DMF removal by the re-suspension steps, the polymer was dissolved in MP-water and lyophilised, to afford the final polymer (143 mg, 99%) as a fluffy, pinkish solid.

^{1}H NMR (400 MHz, DMSO-d_6): δ [ppm] = 8.47–8.37 (m, 2H, C$H_{arom,mTz}$), 7.60–7.40 (m, 2H, C$H_{arom,mTz}$), 4.55–3.75 (m, 198H (2n), br, –NCH_3–CH_2–CO–), 3.10–2.60 (m, 303H (3n), br, –NCH_3).

GPC in HFIP (*vs.* PMMA standards): M_n = 23.8 kg mol^{-1}, $Đ$ = 1.14. Degree of polymerisation (DP) was determined to be 101 by calibration of apparent M_n against a series of pSar standards characterised by static light scattering to obtain absolute molecular weights.[34]

General procedure for the synthesis of TCO-pSar using the example of TCO-pSar$_{66}$. The polymerisation of Sar NCA using *trans*-cyclooctene-amine (TCO-NH_2) as initiator was carried out analogously to the synthesis of mTz-pSar. After lyophilisation, TCO-pSar$_{66}$ was obtained as a colourless solid in quantitative yield.

^{1}H NMR (400 MHz, DMSO-d_6): δ [ppm] = 7.80 (s, 1H, N*H*), 6.94 (s, 1H, N*H*), 5.64–5.36 (m, 2H, –C*H*–C*H*–), 4.72–3.78 (m, 120H (2n), br, –NCH_3–CH_2–CO–), 3.17–2.60 (m, 184H (3n), br, –NCH_3), 2.37–2.15 (m, 4H, –CH_2–), 1.97–1.73 (m, 4H, –CH_2–), 1.70–1.38 (m, 6H, –CH_2–).

GPC in HFIP (*vs.* PMMA standards): M_n = 17.5 kg mol^{-1}, $Đ$ = 1.10. Degree of polymerisation (DP) was determined to be 66 by calibration of apparent M_n against a series of pSar standards characterised by static light scattering to obtain absolute molecular weights.[34]

General procedure for the synthesis of mTz-poly(γ-benzyl-L-glutamate) (mTz-pGlu(OBn)) using the example of mTz-pGlu(OBn)$_{62}$.

Polymerisation of Glu(OBn) NCA using mTz-NH_2 as initiator was carried out at 0 °C analogously to the synthesis of mTz-pSar. Polymer end groups were acetylated by addition of 20 eq. triethylamine and 10 eq. acetic anhydride when complete conversion of the reaction was indicated by IR spectroscopy. The solution was stirred overnight at 0 °C and afterwards precipitated in diethyl ether as described for pSar. mTz-pGlu(OBn)$_{62}$ was obtained as a pink solid in a yield of 99%.

^{1}H NMR (400 MHz, DMSO-d_6): δ [ppm] = 8.81–7.82 (55H (1n), br, N*H*), 7.62–7.52 (m, 2H, C$H_{arom,mTz}$), 7.50–6.94 (m, 305H (5n), –C$H_{arom.}$), 5.30–4.72 (m, 124H (2n), –CH_2–C_6H_5), 4.33–3.70 (m, 62H (1n), NH–C*H*–CO–), 2.98 (s, 3H, –CH_3), 2.42–1.62 (m, 190H (4n), –CH_2–CH_2–).

GPC in HFIP (*vs.* PMMA standards): M_n = 16.2 kg mol^{-1}, $Đ$ = 1.12.

General procedure for the synthesis of TCO-pGlu(OBn) using the example of TCO-pGlu(OBn)$_{23}$. Polymerisation of Glu(OBn) NCA using TCO-NH_2 as initiator was carried out at 0 °C analogously to the synthesis of mTz-pGlu(OBn). TCO-pGlu(OBn)$_{23}$ was obtained as a colourless solid in quantitative yield.

^{1}H NMR (400 MHz, DMSO-d_6): δ [ppm] = 8.55–7.68 (m, 19H (1n), br, N*H*), 7.50–6.94 (m, 112H (5n), –C$H_{arom.}$), 5.64–5.30 (m, 2H, –C*H*–C*H*–), 5.29–4.67 (m, 46H (2n), –CH_2–C_6H_5), 4.22–3.72 (m, 23H (1n), NH–C*H*–CO–), 3.16–2.89 (m, 4H, –CH_2–), 2.45–1.75 (m, 78H (4n), –CH_2–CH_2–), 1.69–1.42 (m, 6H, –CH_2–).

GPC in HFIP (*vs.* PMMA standards): M_n = 9.7 kg mol^{-1}, $Đ$ = 1.15.

mTz-pSar$_{217}$-*b*-p(GluOBn)$_{20}$. The synthesis of mTz-functionalised block copolymers was carried out analogously to the synthesis of mTz-functionalised homopolymers. Briefly, polymerisation of Sar NCA (702 mg, 200 eq.) dissolved in 3.5 mL dry DMF was initiated by addition of mTz-NH_2 (7.25 mg, 1 eq.) from a stock solution in dry DMF and stirred at RT under a constant pressure of 1.25 bar of dry nitrogen. Glu(OBn) NCA (189 mg, 25 eq.) was added to the reaction mixture and stirred at 0 °C after the disappearance of the carbonyl stretching vibration bands at 1850 cm^{-1} and 1780 cm^{-1} of the first monomer indicated complete conversion. Polymer end groups were acetylated by addition of 20 eq. triethylamine and 10 eq. acetic anhydride when complete conversion of the second block was indicated by IR spectroscopy. The solution was stirred overnight at 0 °C and afterwards precipitated in diethyl ether as described for homopolymers. After lyophilisation, mTz-pSar-*b*-pGlu(OBn) was obtained as a pink solid (548 mg, 90% yield).

^{1}H NMR (400 MHz, DMSO-d_6): δ [ppm] = 8.47–8.38 (m, 2H, C$H_{arom,mTz}$), 8.16–7.90 (5H (1n), N*H*), 7.60–7.47 (m, 2H, C$H_{arom,mTz}$), 7.40–7.10 (m, 104H (5n), –C$H_{arom.}$), 5.15–4.85 (m, 40H (2n), –CH_2–C_6H_5), 4.63–3.57 (m, 454H (1n + 2m), NH–C*H*–CO–, –NCH_3–CH_2–CO–), 3.03–2.64 (m, 682H (3m), –NCH_3), 2.42–1.62 (m, 72H (4n), –CH_2–CH_2–).

GPC in HFIP (*vs.* PMMA standards): M_n = 40.2 kg mol^{-1}, $Đ$ = 1.21.

Tetrazine ligations. Polymer stock solutions with a concentration of 1.5 mmol L^{-1} were prepared in MP-water or DMF. Solutions in MP-water were only prepared for polysarcosine homopolymers. 100 μL stock solution of a Tz-functionalised polymer were added to a vial to which 100 μL stock solution of a TCO-functionalised polymer were added and the reaction mixtures were stirred overnight. The next day, aqueous solutions were directly freeze-dried and solutions in DMF were precipitated into diethyl ether and centrifuged (4500 rpm at 4 °C

for 15 min). Polymers were re-suspended in fresh diethyl ether and centrifuged again twice. All polymers were obtained as colourless solids and analysed by GPC in HFIP.

To measure the efficiency and kinetics of the tetrazine ligation by UV–Vis spectroscopy (λ = 540 nm), 70 μL of stock solution of a Tz-functionalised polymer were directly added to a cuvette and measured once. Then, 70 μL of stock solution of a TCO-functionalised polymer at the same concentration were added, mixed with a pipette and measured at the specified time points.

For FCS measurements, Tz-functionalised polymers or nanoparticles were fluorescently labelled using Cy5-TCO. Briefly, Cy5-TCO was added to a hundredfold excess of Tz-functionalised polymer or nanoparticle solution in water from a stock solution, shaken at room temperature for 2 h and stored at 4 °C until measurement. Samples were diluted to a final concentration of 10–100 nM Cy5 prior to measurement.

Nanoparticle preparation

Polymeric micelles. The preparation of polymeric micelles was performed in a similar way as previously described.[30] 100 μL (5 mg) of a 50 mg mL^{-1} stock solution of the mTz-functionalised block copolymer in chloroform were added to a 0.2 mL PCR vial and the chloroform was evaporated overnight. The next day, 50 μL MP-water and 70 mg ceramic beads (SiLibeads ZY-S, 0.3–0.4 mm) were added to the vial and the polymer was allowed to swell for four hours. Centrifugation was performed for 30 min at 3500 rpm with a dual asymmetric centrifuge (SpeedMixer DAC 150.1 CM, Hauschild & Co. KG). After centrifugation, the slightly turbid solution was separated from the beads with an Eppendorf Pipette and the vial was rinsed three times with 50 μL MP-water at a time.

Organic colloids. The preparation of PDLLA-based colloidal nanoparticles was performed in a similar way as previously described.[30] 37.5 mg PDLLA (M_w = 18 000–28 000 g mol^{-1}) were dissolved in 1.25 g chloroform and 10 mg mTz-functionalised block copolymer were dissolved in 3 mL MP-water. The organic phase was added to the aqueous phase and subjected to ultrasonication in a glass vial under ice-cooling for 180 s at 70% amplitude in a pulse regime (10 s sonication, 10 s pause). A Branson Digital Sonifier W-250 with a 1/4″ tip was used for ultrasonication. The obtained miniemulsion was slowly stirred overnight at room temperature until the evaporation of the organic solvent was completed. To separate the nanoparticles from bigger aggregates, the colloidal solution was filtered through syringe filters with a pore size of 1–2 μm (Rotilabo®-fibre glass syringe filters) and afterwards stored at +4 °C or lyophilised. The lyophilised colloids can be re-dissolved before further application.

Results and discussion

In this work, we present a direct synthetic pathway to obtain Tz- and TCO-functionalised polypeptides, polypeptoids and polypept(o)ides by nucleophilic ring-opening polymerisation (ROP), thereby developing new biocompatible polymer systems which can be utilised in tetrazine ligations. The presence of a terminal Tz or TCO group on a polymer allows the introduction of additional functionalities or to synthesise block copolymers. Tz-functionalised amphiphilic block copolypept(o)ides are of particular interest as they can be used to prepare Tz-modified nanoparticles such as polymeric micelles or organic colloids, in which the Tz groups should be easily accessible due to their localization at the end of the corona-forming hydrophilic block. Due to the high reaction rates of tetrazine ligations, nanoparticles bearing the respective functional groups can be quickly functionalised in a bioorthogonal manner, even *in vivo*, which offers interesting possibilities for several diagnostic or therapeutic applications.[39] For example, they could be used as imaging probes in pretargeted imaging approaches or as masking or clearing agents to inactivate or remove unreacted tracer from the circulation.[20,21,40] For these *in vivo* applications, biocompatible and preferably biodegradable polymeric nanoparticles are needed, which is why we chose to use polypept(o)ide-based systems. Scheme 1 provides an overview of the performed syntheses and further application of the synthesised polymers in nanoparticle preparation and ligation experiments. Tz and TCO groups are not only stable during nucleophilic ring-opening polymerisation but moreover easily accessible for post-polymerisation modification.

Polymer synthesis

Polypeptides and polypeptoids can both be synthesised by ROP of *N*-carboxyanhydrides (NCAs) using primary amines as polymerisation initiators. The use of a functional initiator allows the introduction of the respective functional group into the polymer in α-position as long as the respective initiator does not interfere with the polymerisation itself. An alternative route for the incorporation of terminal functionalities is to convert the terminal amino group present in both polymer types into the desired reactive groups by using peptide coupling chemistry. Directly using the functional initiator is usually preferable to any post-polymerisation functionalisation in terms of quantitative end group conversion, as long as the desired group is stable under the polymerisation conditions or suitable protecting groups are available. Amine-functional TCO and commercially available 6-methyl-tetrazine (mTz) were used as initiators in this work. We chose this particular Tz-initiator because methyl-substituted Tz possess high stability in blood serum as compared to more reactive Tz, which are prone to degradation (*e.g.* >90% mTz *vs.* 40% HTz remaining in fetal bovine serum at 37 °C after 10 h).[41] Stability under physiological conditions is an important property with regard to potential *in vivo* applications. Both initiators were dried in high vacuum with azeotropic removal of water with benzene before the polymerisation. Polysarcosine (pSar) as a hydrophilic polypeptoid and poly(γ-benzyl-L-glutamate) (pGlu(OBn)) as hydrophobic polypeptide were synthesised using both initiators respectively. Additionally, the block copolypept(o)ide pSar-*b*-pGlu(OBn) was synthesised bearing an mTz group at

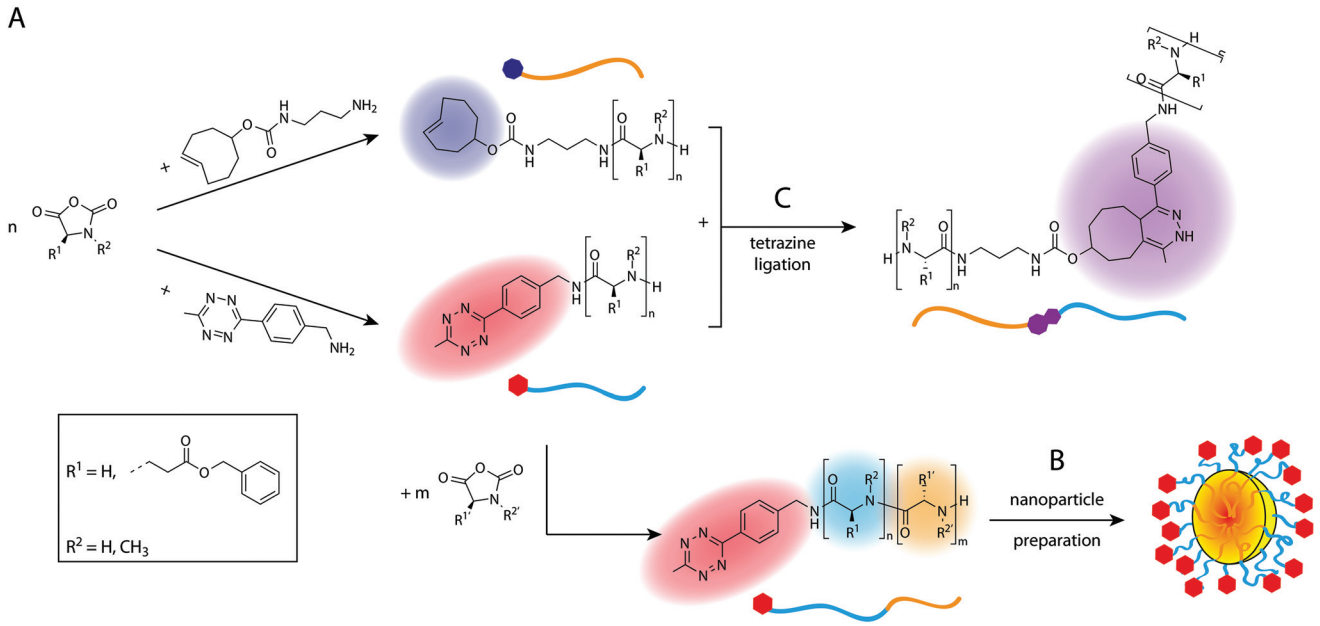

Scheme 1 Overview of polymer synthesis (A) and nanoparticle preparation (B) with subsequent tetrazine ligation experiments (C).

the hydrophilic pSar block. This amphiphilic polymer was further utilised for the preparation of nanoparticles with Tz groups attached to the hydrophilic corona, which could potentially be used as clearing agents in pretargeted imaging. Table 1 gives an overview of all synthesised mTz- and TCO-functionalised polymers.

All polymers were characterised by NMR spectroscopy, GPC and MALDI-TOF mass spectrometry. GPC shows narrow molecular weight distributions for all polymers (Fig. 1), but especially for lower degrees of polymerisation (X_n), the obtained curves have a high molecular weight tailing, which vanishes with increasing polymer length. Interestingly, the tailing is absent in case of amphiphilic block copolymers with a molecular weight of approximately 20 000 g mol^{-1}. It is thus likely that the observed bimodal distributions are due to aggregation behaviour of end group modified polymers in HFIP and not due to side reactions during the polymerisation. Competing initiation by water or other impurities present in the reaction mixture should have an increased impact for polymers with a higher targeted X_n due to the lower amounts of the desired initiator applied. ^{1}H and DOSY NMR spectra confirmed the incorporation of mTz or TCO groups into the polymers (Fig. S1–S7†). Especially for higher X_n, it has to be taken into account, that the determination of the chain length by ^{1}H NMR spectroscopy can be inaccurate due to low intensities of the initiator signals. Thus, the largest difference between X_n observed by GPC and NMR is found for the highest targeted degree of polymerisation of 200. While DOSY confirms that all visible signals of the functional groups possess the same diffusion coefficient and are hence indeed attached to a single

Table 1 Overview of the synthesised mTz- and TCO-functionalised polymers

	Polymer	Initiator	$X_{n(target)}$	$X_{n(MALDI)}$ [a]	$X_{n(NMR)}$ [b]	$X_{n(GPC)}$ [c]	M_n [d] [g mol^{-1}]	$M_{n(GPC)}$ [e] [g mol^{-1}]	$Đ_{(GPC)}$ [e]
P1	pSar	mTz-NH_2	25	23	28	19	1600	8200	1.16
P2	pSar	mTz-NH_2	50	46	53	51	3800	15 300	1.15
P3	pSar	mTz-NH_2	100	82	99	99	7200	23 800	1.14
P4	pSar	mTz-NH_2	200	128	255	179	12 900	27 900	1.26
P5	pSar	TCO-NH_2	50	52	60	66	4900	17 500	1.10
P6	pSar	TCO-NH_2	100	92	113	118	8600	24 000	1.19
P7	pSar	TCO-NH_2	200	130	266	179	12 900	28 100	1.23
P8	pGlu(OBn)	mTz-NH_2	30	30	38	—	8600	10 200	1.12
P9	pGlu(OBn)	mTz-NH_2	60	49	62	—	13 800	16 200	1.12
P10	pGlu(OBn)	TCO-NH_2	25	28	23	—	5300	9700	1.15
P11	pGlu(OBn)	TCO-NH_2	50	58	39	—	8800	21 250	1.16
P12	pSar-*b*-pGlu(OBn)	mTz-NH_2	200/25	—	—/20 [f]	217/—	20 200	40 200	1.21

[a] Highest peak observed in the respective MALDI-TOF spectrum. [b] Determined by ^{1}H NMR spectroscopy in DMSO-d_6. [c] Determined by GPC in HFIP relative to pSar standards. [d] The number average molecular weight calculated from the determined chain lengths. [e] Determined by GPC in HFIP relative to PMMA standards. [f] Determined by ^{1}H NMR spectroscopy in DMSO-d_6 relative to pSar chain length determined by GPC.

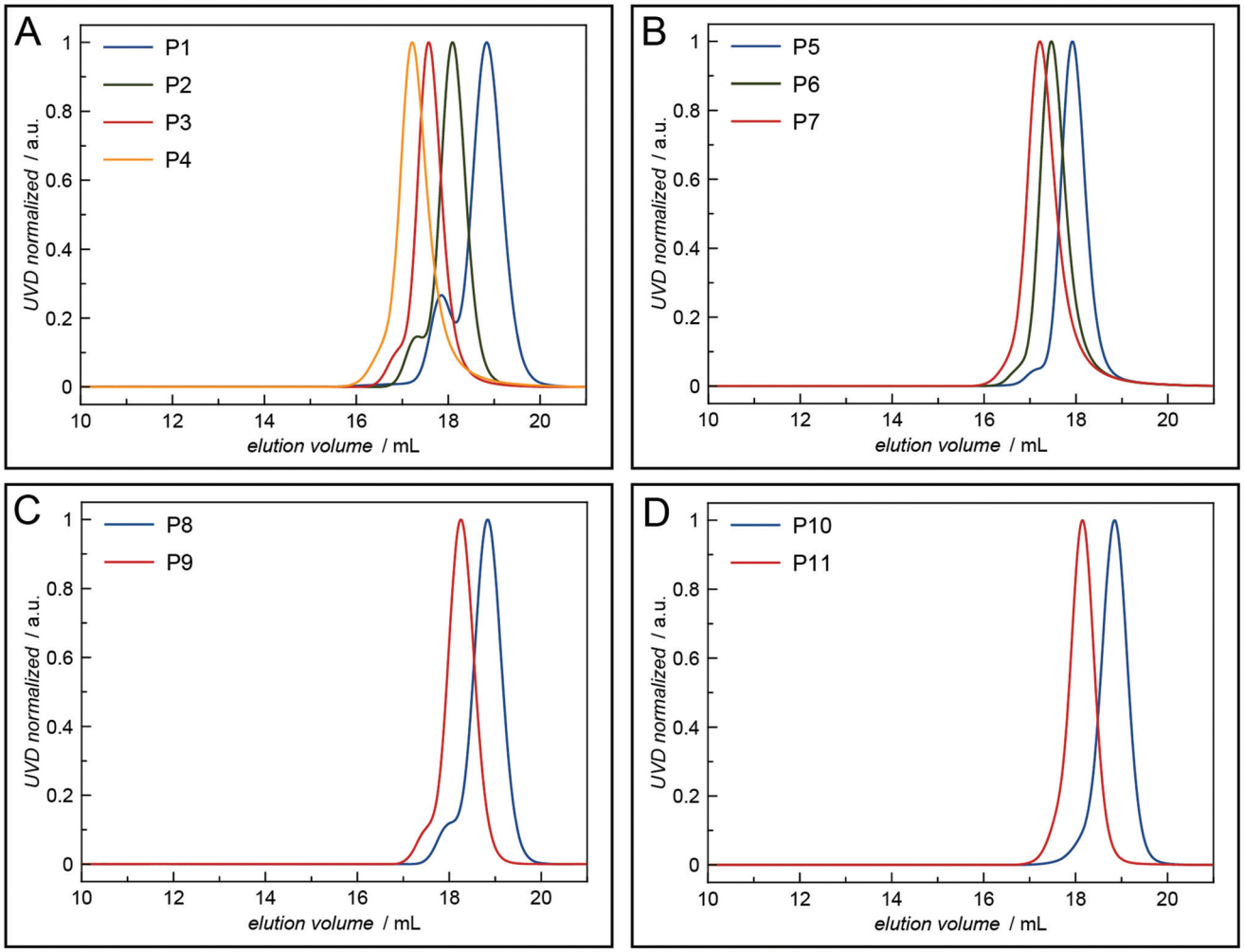

Fig. 1 HFIP GPC elugrams of the synthesised mTz- and TCO-functionalised polymers: (A) mTz-pSar, (B) TCO-pSar, (C) mTz-pGlu(OBn), (D) TCO-pGlu(OBn).

polymer species, it does not prove that all polymer chains bear the desired functionalities. MALDI-TOF mass spectrometry was performed to further analyse the composition of the synthesised polymers, especially with regard to end group integrity, and to analyse the presence of possible side products, *e.g.* polymers initiated by water and thus lacking the functional end group (Fig. 2 and Fig. S12–S15†). All MALDI-TOF spectra show narrow molecular weight distributions with dispersities below 1.03. These values are lower than the dispersities observed with GPC analysis and some are even below the theoretical limit, which is a behaviour sometimes found in MALDI-TOF analysis of polypeptides, polypeptoids and polypept(o)ides caused presumably by mass discrimination effects.[42] More importantly, all peaks could be assigned to the TCO- or mTz-functionalised polymer species that were targeted. The sub-distributions correspond to the same polymer species with different counterions (Fig. S12–S15†). In summary, the combined analytical data underline the successful synthesis of mTz- and TCO-functionalised pSar and pGlu(OBn) and mTz-pSar-*b*-pGlu(OBn) polymers by controlled living nucleophilic ring-opening polymerisation.

Tetrazine ligation experiments

After the synthesis of polymers containing reactive groups, which can be applied to tetrazine ligations with their respective counterparts, it was important to analyse whether these polymers would indeed react both with low molecular weight compounds and also with other polymers to form block copolymers and to which extent reaction kinetics are altered by steric constraints. The synthesis of block copolymers was performed by mixing equimolar solutions of the polymers in DMF, or also in water in the case of the reaction between two pSar polymers, and stirring overnight. GPC analysis demonstrates that for all combinations of pSar and pGlu(OBn) the respective block copolymers can be obtained (Fig. S8–S11†). Minor fractions of remaining homopolymer of one of the reaction partners originate from the fact that for the small amounts of polymer used here, the ratio of the reaction part-

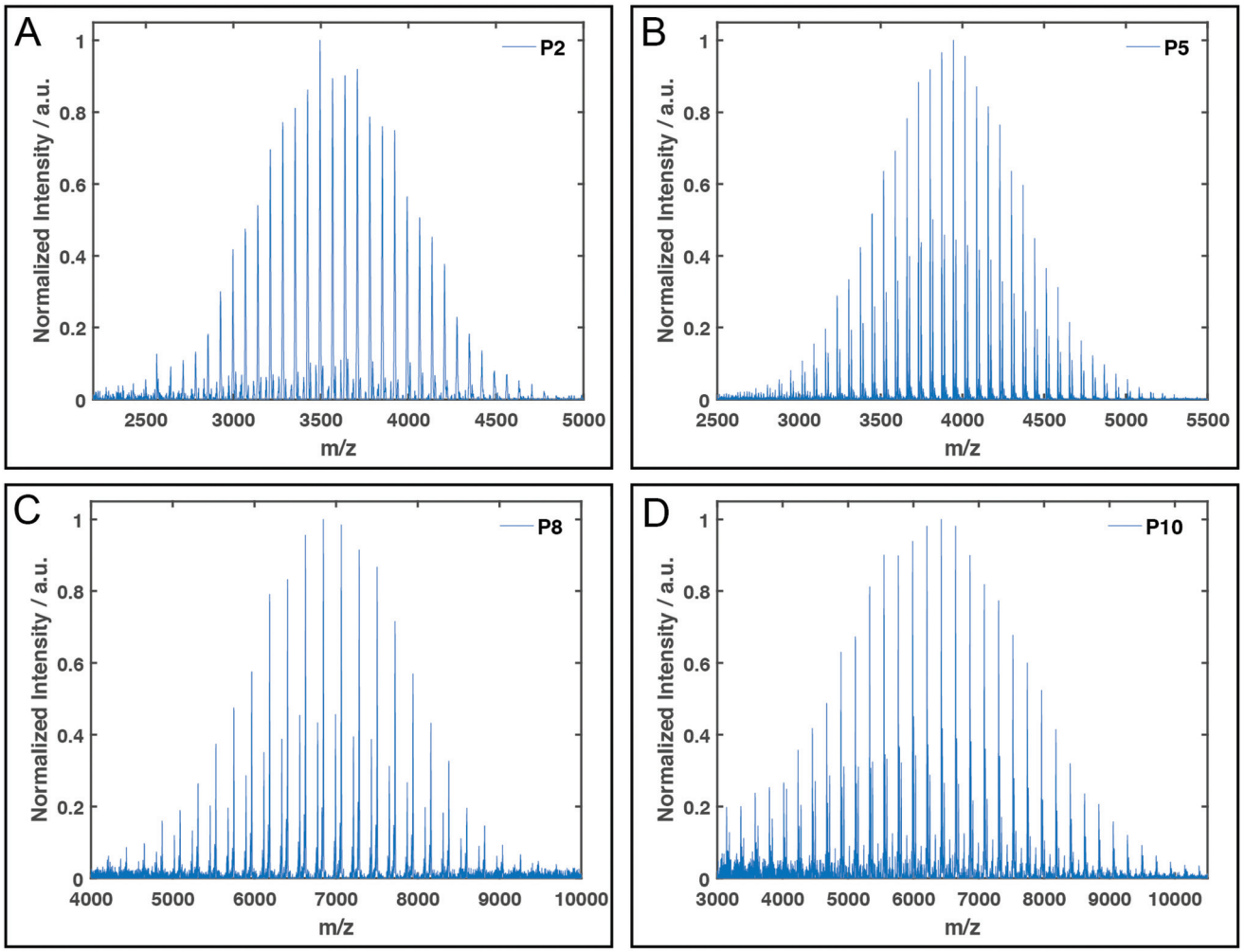

Fig. 2 Exemplary MALDI-TOF plots of mTz-pSar$_{51}$ (P2, A), TCO-pSar$_{66}$ (P5, B), mTZ-pGlu(OBn)$_{38}$ (P8, C) and TCO-pGlu(OBn)$_{23}$ (P10, D).

ners cannot be perfectly adjusted. Moreover, achieving equimolar ratios for both polymers is intrinsically difficult, because molecular weights cannot be accurately determined.

In first experiments, the reaction kinetics of the tetrazine ligation were monitored by UV–Vis spectroscopy using the specific absorption band of the tetrazine group around 530 nm. Briefly, a solution in DMF or water of the Tz-functionalised polymer, to which a solution of TCO-functionalised polymer was added, was analysed at different time points (Fig. S16†).

However, this method with manual addition of the second reactant solution failed to determine second-order rate constants, because the reaction was almost completed already at the first time point at 10 s for reactions in water. Therefore, stopped-flow spectrophotometry was applied to analyse the reaction kinetics of tetrazine ligations between different polymers and low-molecular-weight compounds more accurately. Polymers were reacted among themselves and with TCO-PEG$_4$ or two fluorogenic "turn-on" Tz derivatives (HELIOS 347Me and 388Me;[43] Fig. S17†), which show significantly increased fluorescence upon reaction with a dienophile. This increase in fluorescence allows for real-time monitoring of the reaction progress. Measurements in PBS (pH = 7.4) revealed rates ranging from 463 M^{-1} s^{-1} for the reaction between mTz-pSar$_{20}$ and TCO-PEG$_4$ to 1806 M^{-1} s^{-1} for HELIOS 347Me and TCO-pSar$_{66}$ (Fig. 3A, C and Table 2).

While most reaction rates were in the same range as those of the model reactions between TCO-PEG$_4$ and the two HELIOS Tzs (500–620 M^{-1} s^{-1}), TCO-pSar$_{66}$ reacted significantly faster with both HELIOS Tzs (1500–1800 M^{-1} s^{-1}). We could recently show that the formation of hydrophobic TCO patches on polymer brushes leads to a significant enhancement of reaction rates of the tetrazine ligation.[8] A comparable effect, *i.e.* the formation of micellar assemblies of TCO-pSar, could presumably be the reason for the high reaction rates observed here. Furthermore, conjugation of the hydrophobic TCO to highly hydrophilic pSar could increase the solubility of the TCO compared to TCO-PEG$_4$ and thus allow for faster tetrazine ligation reactions in aqueous media. These results show that Tz and TCO attached to pSar are not only accessible for tetrazine ligation reactions but this combination can even increase the rates of the reaction.

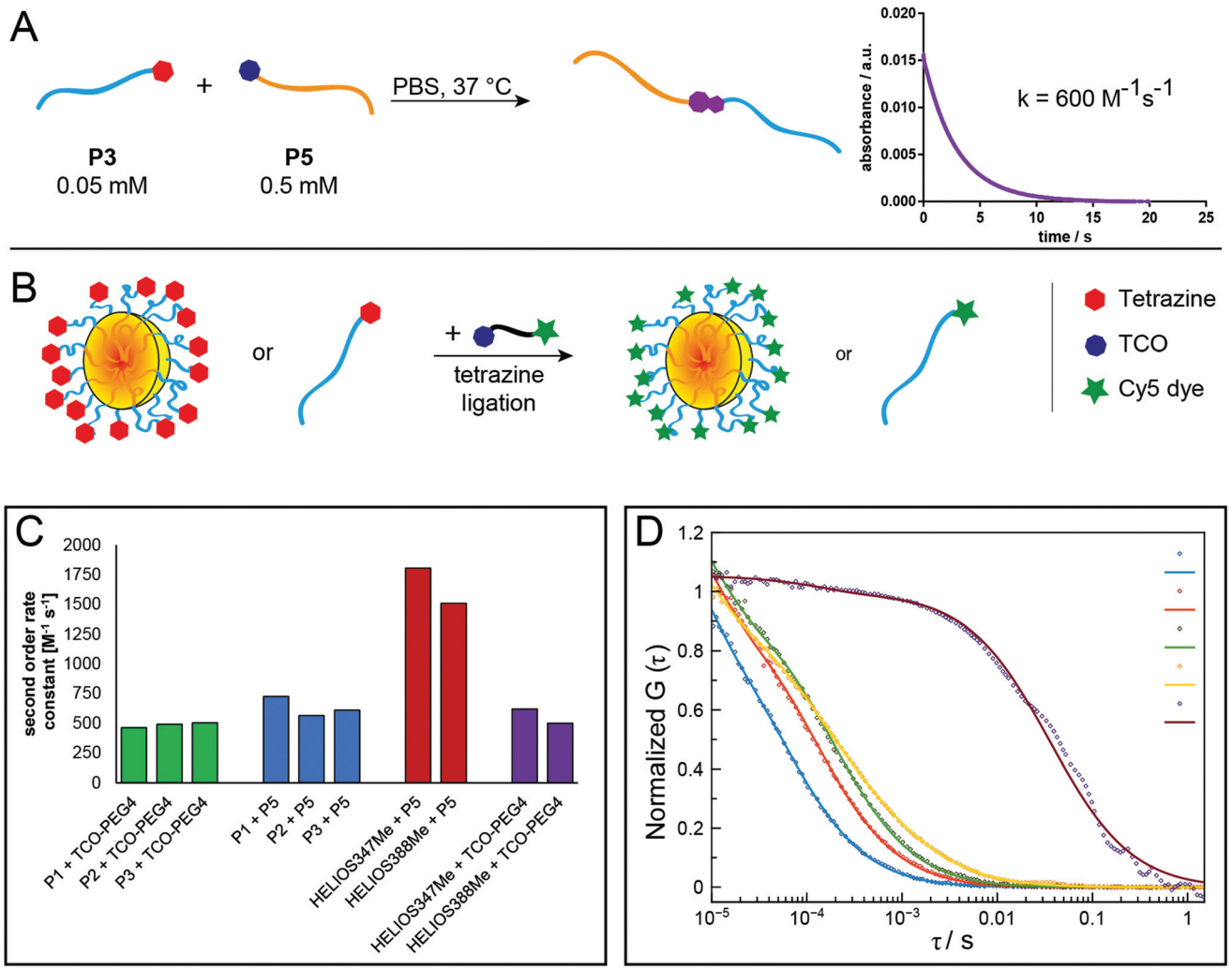

Fig. 3 Schematic representation of the ligation procedure for stopped-flow kinetics measurements with exemplary graph of the reaction rate measurement between **P3** and **P5** (<9 s to 95% conversion, A). Schematic representation of polymer and NP labelling with the fluorescent dye Cy5 prior to FCS measurements (B). Second-order rate constants determined by stopped-flow kinetics measurements (C) and FCS correlation curves after labelling of **P2**, **P4**, polymeric micelles and organic colloids made from **P12** with Cy5-TCO. (D) Squares: measured values, lines: corresponding fits. Blue: Cy5-TCO; Red: **P2**; Green: **P4**; Yellow: polymeric micelles; Purple: colloids.

Table 2 Second-order rate constants of the tetrazine ligation determined by stopped-flow kinetics measurements in PBS at 37 °C

Tz component	TCO component	TCO concentration [mM]	Observed rate [s^{-1}]	k_2 [M^{-1} s^{-1}]	Standard deviation[a] [M^{-1} s^{-1}]
P1	TCO-PEG_4	2.50	1.158	460	0.2
P2	TCO-PEG_4	2.50	1.230	490	0.2
P3	TCO-PEG_4	2.50	1.260	500	0.2
P1	P5	0.55	0.402	730	0.3
P2	P5	0.55	0.313	560	0.6
P3	P5	0.55	0.338	610	0.3
HELIOS 347Me	P5	0.06	0.100	1800	1.2
HELIOS 388Me	P5	0.06	0.084	1500	2.5
HELIOS 347Me	TCO-PEG_4	0.05	0.031	620	0.5
HELIOS 388Me	TCO-PEG_4	0.05	0.025	500	2.3

[a] Values represent the deviation of $n = 3$.

Nanoparticle preparation and conjugation studies

The amphiphilic block copolypept(o)ide mTz-pSar$_{217}$-*b*-pGlu(OBn)$_{20}$ was synthesised to be used in the preparation of two different types of polymeric nanoparticles (NPs), namely polymeric micelles and block copolymer-coated organic colloids (Fig. 4 and Scheme S7†), analogously to the respective non-functional NPs.[30,31] Having the mTz group attached to the hydrophilic pSar block allows for the preparation of NPs with multiple mTz groups attached to the hydrophilic particle corona, which could be useful tools for the attachment of functional moieties *ex* or even *in vivo*. For this purpose, it is important to show whether the Tz groups on the particle surface are still reactive and can be addressed by their TCO counterparts. Therefore, we intended to establish a generally applicable synthesis of polypept(o)ide-based NPs and subsequently investigate their reactivity in tetrazine ligations. Polymeric micelles were prepared by dual asymmetric centrifugation[44] yielding spherical micelles with a z-average hydrodynamic diameter of 112 nm (PDI = 0.15; measured by single-angle DLS) which are on average slightly larger than their non-functionalised analogues (D_h = 102 nm (single-angle DLS)).[30]

mTz-functionalised organic colloids with a core of poly(D,L-lactide) (PDLLA) and mTz-pSar$_{217}$-*b*-pGlu(OBn)$_{20}$ as polymeric surfactant were also obtained in a similar size regime (D_h = 272 nm, PDI = 0.20) as their non-functionalised analogues by miniemulsion technique in combination with solvent evaporation.[31]

Polymeric micelles were additionally analysed by atomic force microscopy (AFM), while organic colloids were visualised by scanning electron microscopy (SEM). Spherical particles could be detected in both cases. The diameter of the polymeric micelles determined from the AFM measurements was in the range of 25 nm to 35 nm and thus considerably smaller than the hydrodynamic diameter determined by single-angle DLS measurements (Fig. 4C). This observation can be attributed to two effects. First, drying effects may occur during sample preparation and a collapse of the corona results in the particles appearing smaller. Secondly, there are some larger particles, possibly compound micelles, which are few in number but contribute disproportionally to the scattering intensities measured by DLS which are proportional to the power of six of the particle radius. SEM images of the organic colloids (Fig. 4D) show a broader particle size distribution in the range of 200–500 nm, also with some larger particles.

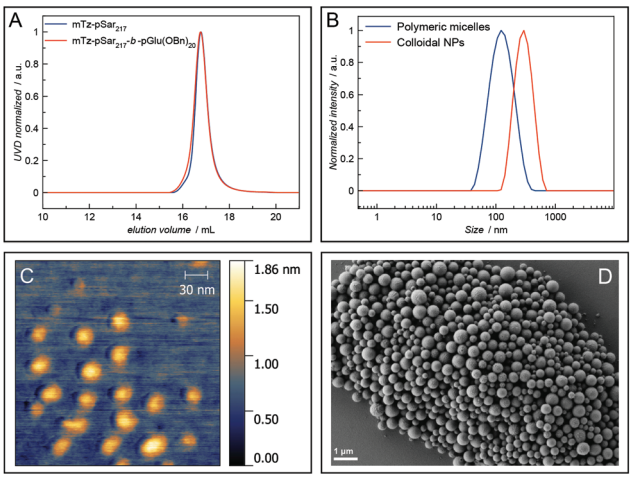

Fig. 4 HFIP GPC elugram of the block copolymer **P12** (A), single-angle DLS plots of polymeric micelles and organic colloids prepared from this polymer (B), AFM image of polymeric micelles (C, scale bar 30 nm) and SEM image of organic colloids (D, scale bar 1 µm).

Fluorescence correlation spectroscopy (FCS) was used to further evaluate the ability of the prepared polymers and NPs to undergo tetrazine ligations. For this purpose, Cy5-TCO was added to polymer or NP samples in aqueous solution and then analysed by FCS. Here, the presence of a fluorescent polymer or nanoparticle species indicates the successful attachment of the fluorescent dye Cy5 to the respective species *via* the tetrazine ligation (Fig. 3B and D). The hydrophilic polymers **P2** and **P4** and the mTz-functional polymeric micelles and organic colloids were reacted with Cy5-TCO in this manner and the respective hydrodynamic radii determined by FCS were 1.4 nm and 2.2 nm for the polymers, 31.2 nm for the polymeric micelles and 134.2 nm for the organic colloids. Thus, the hydrodynamic diameter of the polymeric micelles determined by FCS (62.4 nm) is in between the sizes determined by AFM and single-angle DLS. This value presumably best approximates reality, since with this method the average is determined independent of the particle size and the particle sizes are not altered by drying effects.

The combined results demonstrate that *via* the synthetic pathway established in this work Tz- and TCO-functionalised polypeptides, polypeptoids, polypept(o)ides and Tz-functionalised nanoparticles can be obtained in which the Tz groups are accessible for bioorthogonal tetrazine ligation reactions. Consequently, this approach provides a synthetic route to potential clearing or masking agents for pretargeted nuclear imaging, which are based on the highly biocompatible material polypept(o)ides.

Conclusions

In summary, we present the first synthetic pathway to obtain Tz- or TCO-functionalised polypeptides, polypeptoids and polypept(o)ides by nucleophilic ring-opening polymerisation using the respective functional initiators. Incorporation of the functional groups into well-defined homo- and block copolymers was demonstrated by NMR spectroscopy, GPC and MALDI-TOF mass spectrometry. As the integrity of the reactive groups after the polymerisation process is of great importance for further use of these polymers in bioorthogonal tetrazine ligations, ligation experiments were carried out using the synthesised polymers. The functionalised polymers were shown to react among themselves as well as with small molecules bearing the complementary functionality. Second-order rate constants are within the same order of magnitude or higher as those of low

molecular weight model compounds used in a reference reaction (500–1800 M^{-1} s^{-1}). Additionally, Tz-functionalised polymeric micelles and organic colloids were prepared. These nanoparticles readily reacted with TCO-Cy5 in a model reaction as verified by FCS, indicating stability of the Tz group during the nanoparticle preparation, which enables the fast and efficient modification of nanoparticles by the tetrazine ligation. Future work will be dedicated to determining whether these Tz-functionalised polymers and nanoparticles maintain their reactivity *in vivo* and may be employed as clearing or masking agents in pretargeted nuclear imaging strategies for diagnosis and therapy.

Conflicts of interest

The authors declare no conflict of interest.

Acknowledgements

This project has received funding from the European Union's EU Framework Programme for Research and Innovation Horizon 2020, under grant agreement no. 668532. M. B. acknowledges funding from the CRC 1066-2. This work was supported by the Max Planck Graduate Center with the Johannes Gutenberg-Universität Mainz (MPGC). We thank J. Schnee and S. Türk for assistance with the MALDI-TOF measurements and G. Glaßer for assistance with SEM measurements.

References

1 (*a*) E. M. Sletten and C. R. Bertozzi, *Angew. Chem., Int. Ed.*, 2009, **48**, 6974–6998; (*b*) S. Mayer and K. Lang, *Synthesis*, 2017, **49**, 830–848.

2 N. J. Agard, J. A. Prescher and C. R. Bertozzi, *J. Am. Chem. Soc.*, 2004, **126**, 15046–15047.

3 (*a*) M. L. Blackman, M. Royzen and J. M. Fox, *J. Am. Chem. Soc.*, 2008, **130**, 13518–13519; (*b*) N. K. Devaraj, R. Weissleder and S. A. Hilderbrand, *Bioconjugate Chem.*, 2008, **19**, 2297–2299.

4 A. Darko, S. Wallace, O. Dmitrenko, M. M. Machovina, R. A. Mehl, J. W. Chin and J. M. Fox, *Chem. Sci.*, 2014, **5**, 3770–3776.

5 (*a*) C. Denk, D. Svatunek, T. Filip, T. Wanek, D. Lumpi, J. Fröhlich, C. Kuntner and H. Mikula, *Angew. Chem., Int. Ed.*, 2014, **53**, 9655–9659; (*b*) C. Denk, D. Svatunek, S. Mairinger, J. Stanek, T. Filip, D. Matscheko, C. Kuntner, T. Wanek and H. Mikula, *Bioconjugate Chem.*, 2016, **27**, 1707–1712; (*c*) R. Rossin, S. M. van den Bosch, W. ten Hoeve, M. Carvelli, R. M. Versteegen, J. Lub and M. S. Robillard, *Bioconjugate Chem.*, 2013, **24**, 1210–1217; (*d*) H. Wu and N. K. Devaraj, *Acc. Chem. Res.*, 2018, **51**, 1249–1259; (*e*) M. Wang, R. Vannam, W. D. Lambert, Y. Xie, H. Wang, B. Giglio, X. Ma, Z. Wu, J. Fox and Z. Li, *Chem. Commun.*, 2019, **55**, 2485–2488.

6 Y. Fang, H. Zhang, Z. Huang, S. L. Scinto, J. C. Yang, C. W. am Ende, O. Dmitrenko, D. S. Johnson and J. M. Fox, *Chem. Sci.*, 2018, **9**, 1953–1963.

7 (*a*) R. Rossin, P. R. Verkerk, S. M. van den Bosch, R. C. M. Vulders, I. Verel, J. Lub and M. S. Robillard, *Angew. Chem., Int. Ed.Clin. Cancer Res.*, 2010, **49**, 3375–3378; (*b*) E. J. L. Stéen, P. E. Edem, K. Nørregaard, J. T. Jørgensen, V. Shalgunov, A. Kjaer and M. M. Herth, *Biomaterials*, 2018, **179**, 209–245; (*c*) S. Poty, L. M. Carter, K. Mandleywala, R. Membreno, D. Abdel-Atti, A. Ragupathi, W. W. Scholz, B. M. Zeglis and J. S. Lewis, *Clin. Cancer Res.*, 2019, **25**, 868–880; (*d*) R. Membreno, B. E. Cook, K. Fung, J. S. Lewis and B. M. Zeglis, *Mol. Pharmaceutics*, 2018, **15**, 1729–1734.

8 E. J. L. Stéen, J. T. Jørgensen, K. Johann, K. Norregaard, B. Sohr, D. Svatunek, A. Birke, V. Shalgunov, P. E. Edem, R. Rossin, C. Seidl, F. Schmid, M. S. Robillard, J. L. Kristensen, H. Mikula, M. Barz, A. Kjaer, M. M. Herth, K. Nørregaard and A. Kjær, *ACS Nano*, 2020, **14**, 568–584.

9 M. Pagel, *J. Pept. Sci.*, 2019, **25**, e3141.

10 J. W. Wollack, B. J. Monson, J. K. Dozier, J. J. Dalluge, K. Poss, S. A. Hilderbrand and M. D. Distefano, *Chem. Biol. Drug Des.*, 2014, **84**, 140–147.

11 H. Koo, M. Choi, E. Kim, S. K. Hahn, R. Weissleder and S. H. Yun, *Small*, 2015, **11**, 6458–6466.

12 (*a*) R. Rossin, S. M. J. van Duijnhoven, W. ten Hoeve, H. M. Janssen, L. H. J. Kleijn, F. J. M. Hoeben, R. M. Versteegen and M. S. Robillard, *Bioconjugate Chem.*, 2016, **27**, 1697–1706; (*b*) R. M. Versteegen, W. ten Hoeve, R. Rossin, M. A. R. de Geus, H. M. Janssen and M. S. Robillard, *Angew. Chem., Int. Ed.*, 2018, **57**, 10494–10499; (*c*) R. M. Versteegen, R. Rossin, W. ten Hoeve, H. M. Janssen and M. S. Robillard, *Angew. Chem., Int. Ed.*, 2013, **52**, 14112–14116; (*d*) J. C. T. Carlson, H. Mikula and R. Weissleder, *J. Am. Chem. Soc.*, 2018, **140**, 3603–3612.

13 I. A. Barker, D. J. Hall, C. F. Hansell, F. E. Du Prez, R. K. O'Reilly and A. P. Dove, *Macromol. Rapid Commun.*, 2011, **32**, 1362–1366.

14 R. J. Williams, I. A. Barker, R. K. O'Reilly and A. P. Dove, *ACS Macro Lett.*, 2012, **1**, 1285–1290.

15 C. F. Hansell, P. Espeel, M. M. Stamenović, I. A. Barker, A. P. Dove, F. E. Du Prez and R. K. O'Reilly, *J. Am. Chem. Soc.*, 2011, **133**, 13828–13831.

16 L. Xu, M. Raabe, M. M. Zegota, J. Nogueira, V. Chudasama, S. L. Kuan, T. Weil, M. M. Zegota and J. C. F. Nogueira, *Org. Biomol. Chem.*, 2020, **18**, 1140–1147.

17 M. M. Lorenzo, C. G. Decker, M. U. Kahveci, S. J. Paluck and H. D. Maynard, *Macromolecules*, 2016, **49**, 30–37.

18 O. Roling, A. Mardyukov, S. Lamping, B. Vonhören, S. Rinnen, H. F. Arlinghaus, A. Studer and B. J. Ravoo, *Org. Biomol. Chem.*, 2014, **12**, 7828–7835.

19 (*a*) N. K. Devaraj, G. M. Thurber, E. J. Keliher, B. Marinelli and R. Weissleder, *Proc. Natl. Acad. Sci. U. S. A.*, 2012, **109**, 4762–4767; (*b*) R. Membreno, O. M. Keinänen, B. E. Cook, K. M. Tully, K. C. Fung, J. S. Lewis and B. M. Zeglis, *Mol. Pharmaceutics*, 2019, **16**, 2259–2263.

20 J.-P. Meyer, K. M. Tully, J. Jackson, T. R. Dilling, T. Reiner and J. S. Lewis, *Bioconjugate Chem.*, 2018, **29**, 538–545.
21 R. Rossin, T. Läppchen, S. M. van den Bosch, R. Laforest and M. S. Robillard, *J. Nucl. Med.*, 2013, **54**, 1989–1995.
22 S. S. Kara, M. Y. Ateş, G. Deveci, A. Cetinkaya and M. U. Kahveci, *J. Polym. Sci., Part A: Polym. Chem.*, 2019, **57**, 673–680.
23 S. Kramer, D. Svatunek, I. Alberg, B. Gräfen, S. Schmitt, L. Braun, A. H. A. M. van Onzen, R. Rossin, K. Koynov, H. Mikula and R. Zentel, *Biomacromolecules*, 2019, **20**, 3786–3797.
24 (*a*) T. Aliferis, H. Iatrou and N. Hadjichristidis, *Biomacromolecules*, 2004, **5**, 1653–1656; (*b*) T. J. Deming, *J. Polym. Sci., Part A: Polym. Chem.*, 2000, **38**, 3011–3018; (*c*) N. Hadjichristidis, H. Iatrou, M. Pitsikalis and G. Sakellariou, *Chem. Rev.*, 2009, **109**, 5528–5578; (*d*) T. J. Deming, *Adv. Mater.*, 1997, **9**, 299–311; (*e*) *Peptide-Based Materials*, ed. T. Deming, Springer Berlin Heidelberg, Berlin, Heidelberg, 2012; (*f*) A. Duro-Castano, I. Conejos-Sánchez and M. Vicent, *Polymers*, 2014, **6**, 515–551.
25 C. Bonduelle, *Polym. Chem.*, 2018, **9**, 1517–1529.
26 (*a*) A. Birke, J. Ling and M. Barz, *Prog. Polym. Sci.*, 2018, **81**, 163–208; (*b*) C. Fetsch, A. Grossmann, L. Holz, J. F. Nawroth and R. Luxenhofer, *Macromolecules*, 2011, **44**, 6746–6758; (*c*) R. Luxenhofer, C. Fetsch and A. Grossmann, *J. Polym. Sci., Part A: Polym. Chem.*, 2013, **51**, 2731–2752; (*d*) C. Secker, S. M. Brosnan, R. Luxenhofer and H. Schlaad, *Macromol. Biosci.*, 2015, **15**, 881–891; (*e*) B. A. Chan, S. Xuan, A. Li, J. M. Simpson, G. L. Sternhagen, T. Yu, O. A. Darvish, N. Jiang and D. Zhang, *Biopolymers*, 2018, **109**, e23070; (*f*) D. Zhang, S. H. Lahasky, L. Guo, C.-U. Lee and M. Lavan, *Macromolecules*, 2012, **45**, 5833–5841; (*g*) N. Gangloff, J. Ulbricht, T. Lorson, H. Schlaad and R. Luxenhofer, *Chem. Rev.*, 2016, **116**, 1753–1802.
27 J. Sun and R. N. Zuckermann, *ACS Nano*, 2013, **7**, 4715–4732.
28 K. Klinker and M. Barz, *Macromol. Rapid Commun.*, 2015, **36**, 1943–1957.
29 P. Heller, A. Birke, D. Huesmann, B. Weber, K. Fischer, A. Reske-Kunz, M. Bros and M. Barz, *Macromol. Biosci.*, 2014, **14**, 1380–1395.
30 F. Fenaroli, U. Repnik, Y. Xu, K. Johann, S. van Herck, P. Dey, F. M. Skjeldal, D. M. Frei, S. Bagherifam, A. Kocere, R. Haag, B. G. de Geest, M. Barz, D. G. Russell and G. Griffiths, *ACS Nano*, 2018, **12**, 8646–8661.
31 A. Birke, D. Huesmann, A. Kelsch, M. Weilbächer, J. Xie, M. Bros, T. Bopp, C. Becker, K. Landfester and M. Barz, *Biomacromolecules*, 2014, **15**, 548–557.
32 (*a*) R. Holm, K. Klinker, B. Weber and M. Barz, *Macromol. Rapid Commun.*, 2015, **36**, 2083–2091; (*b*) P. Heller, B. Weber, A. Birke and M. Barz, *Macromol. Rapid Commun.*, 2015, **36**, 38–44; (*c*) C. Deng, J. Wu, R. Cheng, F. Meng, H.-A. Klok and Z. Zhong, *Prog. Polym. Sci.*, 2014, **39**, 330–364.
33 K. Klinker, R. Holm, P. Heller and M. Barz, *Polym. Chem.*, 2015, **6**, 4612–4623.
34 B. Weber, A. Birke, K. Fischer, M. Schmidt and M. Barz, *Macromolecules*, 2018, **51**, 2653–2661.
35 (*a*) P. H. Maurer, D. Subrahmanyam, E. Katchalski and E. R. Blout, *J. Immunol.*, 1959, **83**, 193–197; (*b*) M. Sela, *Adv. Immunol.*, 1966, **5**, 29–129; (*c*) S. Bleher, J. Buck, C. Muhl, S. Sieber, S. Barnert, D. Witzigmann, J. Huwyler, M. Barz and R. Süss, *Small*, 2019, e1904716; (*d*) B. Steinborn, P. Hirschle, M. Höhn, T. Bauer, M. Barz, S. Wuttke, E. Wagner and U. Lächelt, *Adv. Ther.*, 2019, **2**, 1900120; (*e*) I. Negwer, A. Best, M. Schinnerer, O. Schäfer, L. Capeloa, M. Wagner, M. Schmidt, V. Mailänder, M. Helm, M. Barz, H.-J. Butt and K. Koynov, *Nat. Commun.*, 2018, **9**, 5306; (*f*) A. Zimpel, N. Al Danaf, B. Steinborn, J. Kuhn, M. Höhn, T. Bauer, P. Hirschle, W. Schrimpf, H. Engelke, E. Wagner, M. Barz, D. C. Lamb, U. Lächelt and S. Wuttke, *ACS Nano*, 2019, **13**, 3884–3895.
36 E. Ostuni, R. G. Chapman, R. E. Holmlin, S. Takayama and G. M. Whitesides, *Langmuir*, 2001, **17**, 5605–5620.
37 (*a*) D. Huesmann, K. Klinker and M. Barz, *Polym. Chem.*, 2017, **8**, 957–971; (*b*) T. J. Deming, *Chem. Rev.*, 2016, **116**, 786–808; (*c*) Z. Song, H. Fu, R. Wang, L. A. Pacheco, X. Wang, Y. Lin and J. Cheng, *Chem. Soc. Rev.*, 2018, **47**, 7401–7425; (*d*) Z. Song, Z. Han, S. Lv, C. Chen, L. Chen, L. Yin and J. Cheng, *Chem. Soc. Rev.*, 2017, **46**, 6570–6599; (*e*) J. Huang and A. Heise, *Chem. Soc. Rev.*, 2013, **42**, 7373–7390.
38 R. Rigler and E. S. Elson, *Fluorescence Correlation Spectroscopy. Theory and Applications*, Springer, Berlin, Heidelberg, 2001, vol. 65.
39 (*a*) H. J. Chung, T. Reiner, G. Budin, C. Min, M. Liong, D. Issadore, H. Lee and R. Weissleder, *ACS Nano*, 2011, **5**, 8834–8841; (*b*) V. M. Peterson, C. M. Castro, H. Lee and R. Weissleder, *ACS Nano*, 2012, **6**, 3506–3513; (*c*) J. B. Haun, N. K. Devaraj, S. A. Hilderbrand, H. Lee and R. Weissleder, *Nat. Nanotechnol.*, 2010, **5**, 660–665.
40 (*a*) S. M. J. van Duijnhoven, R. Rossin, S. M. van den Bosch, M. P. Wheatcroft, P. J. Hudson and M. S. Robillard, *J. Nucl. Med.*, 2015, **56**, 1422–1428; (*b*) M. F. García, X. Zhang, M. Shah, J. Newton-Northup, P. Cabral, H. Cerecetto and T. Quinn, *Bioorg. Med. Chem.*, 2016, **24**, 1209–1215; (*c*) B. M. Zeglis, C. Brand, D. Abdel-Atti, K. E. Carnazza, B. E. Cook, S. Carlin, T. Reiner and J. S. Lewis, *Mol. Pharmaceutics*, 2015, **12**, 3575–3587; (*d*) D. Summer, S. Mayr, M. Petrik, C. Rangger, K. Schoeler, L. Vieider, B. Matuszczak and C. Decristoforo, *Pharmaceuticals*, 2018, **11**, 102.
41 M. R. Karver, R. Weissleder and S. A. Hilderbrand, *Bioconjugate Chem.*, 2011, **22**, 2263–2270.
42 (*a*) C. Muhl, O. Schäfer, T. Bauer, H.-J. Räder and M. Barz, *Macromolecules*, 2018, **51**, 8188–8196; (*b*) D. Huesmann, A. Birke, K. Klinker, S. Türk, H. J. Räder and M. Barz, *Macromolecules*, 2014, **47**, 928–936.
43 L. G. Meimetis, J. C. T. Carlson, R. J. Giedt, R. H. Kohler and R. Weissleder, *Angew. Chem., Int. Ed.*, 2014, **53**, 7531–7534.
44 (*a*) B. Weber, C. Kappel, M. Scherer, M. Helm, M. Bros, S. Grabbe and M. Barz, *Macromol. Biosci.*, 2017, **17**, 1700061; (*b*) U. Massing, S. Cicko and V. Ziroli, *J. Controlled Release*, 2008, **125**, 16–24.